Mapping cardiogenic oscillations using synchrotron based phase contrast CT imaging

Jordan Thurgood*[a], Stephen Dubsky[a], Karen K W Siu[b], Megan Wallace[c], Melissa Siew[c], Stuart Hooper[c], Andreas Fouras[a]
[a]Laboratory for Dynamic Imaging, Department of Mechanical and Aerospace Engineering, Monash, University, Clayton, VIC 3800, Australia; [b]School of Physics, Monash University, Clayton, VIC 3800, Australia; [c]Ritchie Centre, Monash Institute of Medical Research, Monash University, Clayton, VIC 3800, Australia

ABSTRACT

In many animals, including humans, the lungs encase the majority of the heart thus the motion of each organ affects the other. The effects of the motion of the heart on the lungs potentially provides information with regards to both lung and heart health. We present a novel technique that is capable of measuring the effect of the heart on the surrounding lung tissue through the use of advanced synchrotron imaging techniques and recently developed X-ray velocimetry methods. This technique generates 2D frequency response maps of the lung tissue motion at multiple projection angles from projection X-ray images. These frequency response maps are subsequently used to generate 3D reconstructions of the lung tissue exhibiting motion at the frequency of ventilation and the lung tissue exhibiting motion at the frequency of the heart. This technique has a combined spatial and temporal resolution sufficient to observe the dynamic and complex 3D nature of lung-heart interactions.

Keywords: Cardiogenic oscillations, cardiogenic mixing, heart imaging, lung imaging, synchrotron, ventilation, x-ray velocimetry, computed tomography.

1. INTRODUCTION

1.1 Lung-Heart Interactions

The heart and lungs are intimately connected systems, the function of both being critical for survival. Each system inherently affects the other due to the lungs encasing the heart. As the heart contracts and expands to pump blood, it induces motion in the lung tissue directly adjacent to it. This motion of the lung tissue resulting from the heart is known as cardiogenic oscillations. Cardiogenic oscillations are believed to produce a mixing of the gas within the lungs [1, 2] as well as a global flow of gas into and out of the lung.

Lung-heart interactions are complex in nature due to multiple factors including the complexity of the heart contraction cycle, large lung tissue motions induced from respiration as well as these two systems operating at differing frequencies. Not only are these interactions complex in their nature but they are also occurring at very fast rates, especially in small animal models. For instance a mouse heart typically beats on the order of 500 times per minute, therefore techniques looking at the heart's effect on the lungs must be able to resolve very high frequencies.

Cardiogenic oscillations have been studied due to their effect on auto-triggering ventilators, especially in the case of brain dead patients[3]. Yet cardiogenic oscillations have also been postulated to be potentially useful measures of lung compliance[4-6] and central apnea[7]. Cardiogenic oscillations are known to have an effect on aerosol delivery and dispersion during breath holding[8]. It has been shown that pulmonary blood flow and volume can affect cardiogenic oscillations measured at the airway opening[9, 10], yet the authors believe the physical motion of the heart on the surrounding lung tissue also has a great effect.

Previous methods for investigating cardiogenic oscillations can be separated into two distinct groups: temporally resolved methods and spatially resolved methods. Temporally resolved methods for investigating cardiogenic

Developments in X-Ray Tomography VIII, edited by Stuart R. Stock,
Proc. of SPIE Vol. 8506, 85060H · © 2012 SPIE · CCC code: 0277-786/12/$18
doi: 10.1117/12.929463

oscillations have included measuring electrical impedance[11], expired gas concentration[12] and airway flow[9, 13] yet these methods are all lacking in regional information of lung-heart interactions. Spatially resolved methods for imaging of the lungs and heart, such as computed tomography (CT) and magnetic resonance imaging (MRI), suffer from long acquisition times and are not capable of resolving the temporal nature of lung-heart interactions. There is a need for measurement techniques that can fully resolve the complex motion occurring during cardiogenic oscillations due to effects such as destructive interference[14], as well as the ability for these techniques to be used at very high acquisition rates.

1.2 Synchrotron imaging

Synchrotrons provide coherent and high brilliance X-rays and have recently allowed great advancements with regards *in vivo* lung imaging[15, 16]. As coherent X-rays propagate through the chest of a subject they interact with the many air-tissue boundaries present within the lung. At each of these boundaries the X-rays refract marginally, yet with sufficient propagation distance to the detector these interactions can become evident. By exploiting this property of coherent X-ray radiation, phase contrast imaging can provide highly detailed images of the lung with excellent contrast[17]. Figure 1 illustrates the setup for this imaging procedure which has been developed for high speed imaging of the entire lung field, achieving rates of up to 300fps[18].

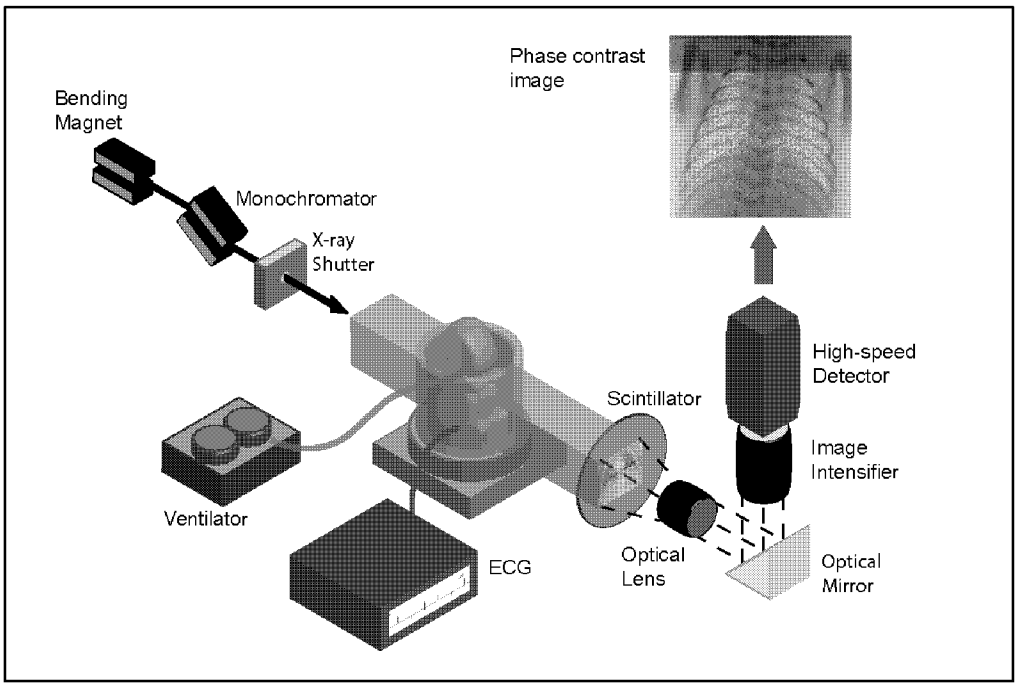

Figure 1. The experimental set-up used for capturing high resolution and high contrast synchrotron based phase contrast images of the mouse lung at frame rates of up to 300fps.

1.3 X-ray Velocimetry

High contrast and high-resolution images that are generated using the above synchrotron imaging method provide an excellent base for use in an X-ray velocimetry analysis[19, 20]. The images are divided into rectangular interrogation regions upon which a cross-correlation analysis is performed between subsequent frames. The peak of the cross-correlation is the statistically most likely displacement of the tissue within that region at that instant in time. Each interrogation region results in a single vector that describes the magnitude and direction of tissue displacement within that region at that particular moment in time, as seen in Figure 2. X-ray velocimetry allows for accurate measurements of both spatial and temporal variations in lung tissue motion.

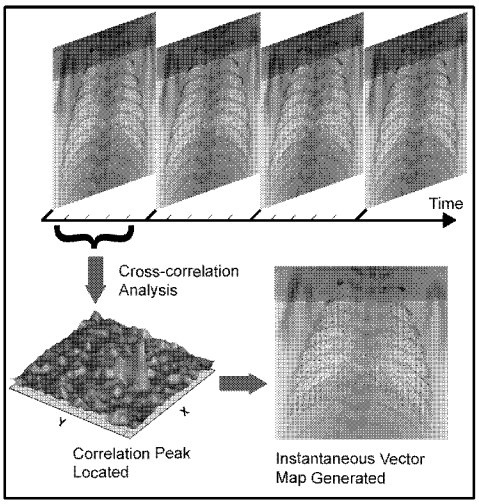

Figure 2. X-ray velocimetry analysis process utilised to determine region displacements of lung tissue between subsequent frames. Images are divided into interrogation regions upon which a cross-correlation is performed with the same region in the subsequent frame. The correlation peak is the statistically most likely displacement of lung tissue within that region at that instant in time.

2. METHODS

2.1 Animal Procedures

C57BL6 adult male mice (10-12 weeks old) were anaesthetised with somnopentyl (pentobarbitone sodium; i.p.; 70mg/kg) and orally intubated with a suitable endotracheal tube (20G). Mice were then positioned upright in a custom-made imaging sample mount located in the X-ray beam path within the imaging hutch. Anaesthesia was maintained during imaging using a constant infusion of pentobarbitone sodium (somnopentyl; i.p.; 0.012mg/min). An ECG was connected to the subject for monitoring purposes and for validation of the heart rate. Animals were connected to a custom designed pressure-controlled ventilator[21]. Ventilation was maintained with an inspiratory time of 135 ms with a positive inspiratory pressure of 14 cmH_2O and an expiratory time of 265 ms with an end-expiratory pressure of 2 cmH_2O equating to a ventilation frequency of 2.5 Hz (150 breaths per minute).

2.2 Imaging Procedures

The experiments were performed in hutch 3 of beamline 20B2 in the Biomedical Imaging Centre of the SPring-8 synchrotron in Kyoto, Japan. A monochromator was used to selectively tune the radiation energy to 30KeV. A PCO Edge sCMOS camera was used with a 50μm thick P43 powder based scintillator on an X-ray converter (Hamamatsu BM5) as the detector setup, see Figure 1. Images were recorded at 50fps with 20 images per breath, triggered from the start of inspiration. Figure 3A shows an example of a phase contrast image generated from this imaging setup.

7515 images were recorded as the subject was rotated through 180 degrees. Images were flat field corrected[22] and a spatial frequency filter was applied to improve the image quality for the X-ray velocimetry analysis. The image sequence was divided in to blocks of 150 images (3.6 degrees of rotation), each with an overlap of 130 images on the previous, thus creating 368 imaging blocks with a rotation angle of 0.5 degrees between each image block. An X-ray velocimetry analysis was performed on each imaging block using in-house software[23] with interrogation regions of 64 x 64 pixels with an overlap of 8 pixels. This software uses an implementation of sub-pixel interpolation and has been thoroughly evaluated and found to have a practical error limit of approximately 0.05 pixels[24]. Figure 3B shows a vector map indicating the instantaneous motion of lung tissue between the subsequent images during a breath hold, caused by the heart motion. Vectors are coloured according to magnitude of motion, with red indicating largest instantaneous displacement and blue the smallest. Only a sixteenth of all vectors displayed for clarity purposes.

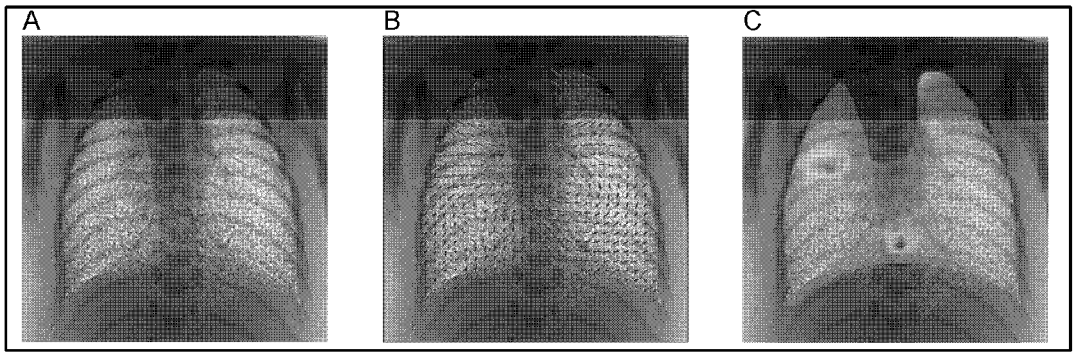

Figure 3. A) High resolution and high contrast image obtained from the synchrotron based phase contrast imaging method. B) Vector map of the instantaneous motion due to the heart's action during a breath hold. Vectors are coloured according to magnitude of motion, with red indicating largest instantaneous displacement and blue the smallest. Only 1/16 of all vectors are shown for clarity. C) Contour map displaying power of motion at the frequency of the heart beat. The distinct areas of lung tissue affected by the atria and ventricles are easily located within this image.

2.3 Frequency analysis

For each imaging block of 150 images the results of the X-ray velocimetry analysis were used to determine the amplitude of motion at both the ventilation frequency (2.5 Hz) and the heart frequency (6.5 Hz). An FFT analysis of each vector was performed to obtain the frequency response of each location for a particular projection angle and a map of the amplitude for each frequency was generated. This resulted in 368 frequency response projection maps for both the ventilation and heart frequencies as the subject was rotated through 180 degrees. Figure 3C shows a frequency response projection map for a single frontal view. These 368 frequency response projection maps are then used to reconstruct 3D renderings of the amplitude of motion of the lungs at both the ventilation frequency and at the heart frequency. An FFT analysis was also performed on the ECG trace for validation of the frequency of the heart.

2.4 CT reconstruction

The frequency response projection maps generated from the FFT analysis of each location in the X-ray velocimetry data were used as 368 individual projections from which a CT reconstruction was performed. A CT reconstruction was also performed on the original images to generate a high-resolution 3D render of the subject's lungs, Figure 4. The images were placed into one of 20 bins depending on their temporal location on the respiratory cycle. This resulted in 20 individual reconstructions throughout the breath, each reconstruction being composed of 375 different projection images. Both CT reconstructions were performed using a simultaneous algebraic reconstruction technique and were performed on a GPU processor using in-house software.

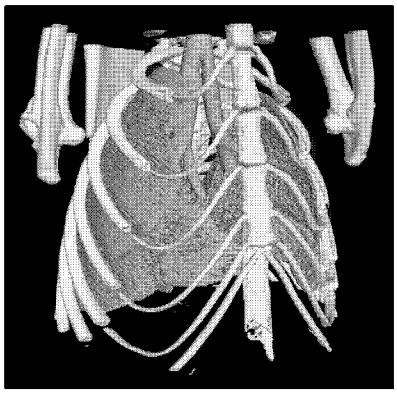

Figure 4. CT reconstruction of mouse lung generated using 376 projection images from the same point in the ventilation cycle. The lung tissue is false coloured blue and the bone white. Image courtesy S. Dubsky [16].

3. RESULTS AND DISCUSSION

When performing an expiratory breath hold, pressure oscillations were induced onto the lung via the heart and could often be measured at the airway opening, as shown in Figure 5. These oscillations were well aligned with the ECG trace confirming their origins to be from the heart. However the oscillations were not always present, highlighting the need for further study into the origin and function of cardiogenic oscillations.

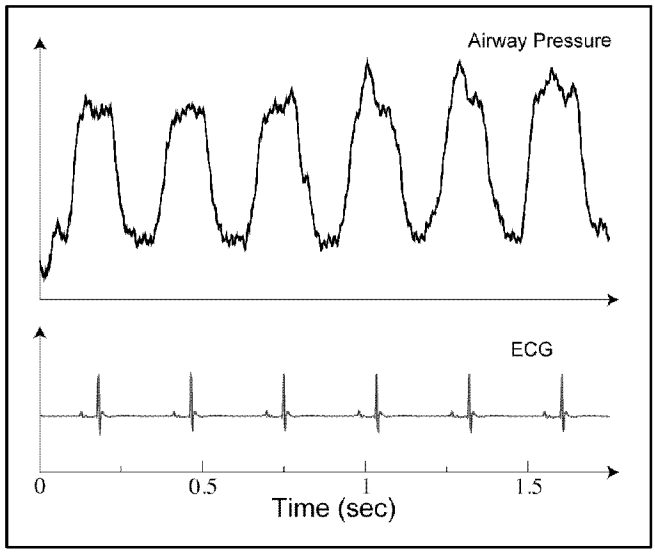

Figure 5. Upper) A pressure trace recorded at the airway opening during an end-expiratory breath-hold manoeuvre on a mouse. Cardiogenic oscillations within the animal are evident here as pressure oscillations at the airway opening. Lower) ECG trace recorded simultaneously with the pressure recording showing the relationship between the heart and the pressure fluctuations measured at the airway opening.

The frequency response plots confirmed that there were multiple frequencies present in the motion of the lung tissue. Figure 6 shows the frequencies that were measured by X-ray velocimetry on one particular animal. There are clear peaks around the ventilation frequency (2.5Hz) and its second harmonic (5 Hz) as well as at the heart frequency (6.5 Hz). The ECG confirmed the heart frequency to be 6.5 Hz.

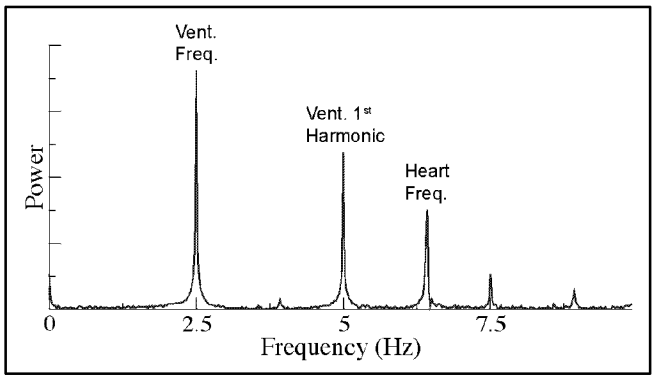

Figure 6. Plot of the frequency response of X-ray velocimetry data for one animal. There are well-defined peaks at the ventilation frequency (2.5Hz), the second harmonic of the ventilation frequency (5Hz) and at the frequency of the heart (6.5Hz). The ventilation peak can be seen to be much stronger than that of the heart. This is calculated off the spatial average of all vectors within each image.

A 3D reconstruction of the 368 frequency response projection maps is shown in Figure 7A. The structure of the lung can be clearly seen in the reconstruction, indicating that ventilation affects lung motion across the entire lung. The reconstructions at the ventilation frequency and the heart frequency are shown in different colours overlaid on one

another in Figure 7B. The heart's effect on lung motion is noted to be predominantly around the various chambers of the heart, the atria and ventricles. The atria affected the lung tissue in the apex of each side respectively and the ventricles affect lung tissue in the region surrounding the lower portion of the heart. Distal to the heart there was minimal lung tissue motion observed at the frequency of the heart. The analysis for the heart frequency and the ventilation frequency is performed on the same image data set that was acquired at a frame rate much faster than the heart frequency, highlighting the strengths of this technique.

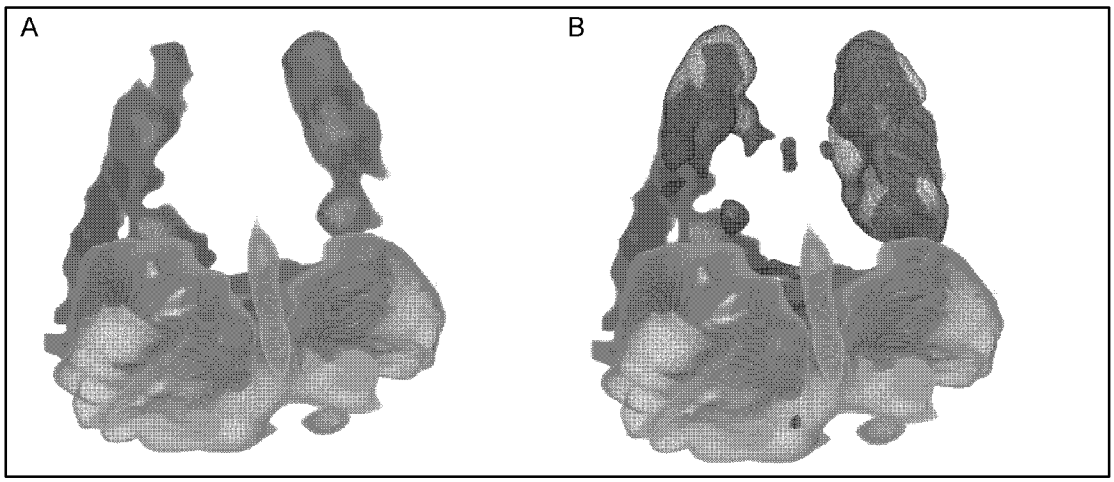

Figure 7. A) Rendering of the reconstruction of the frequency response projection images at the ventilation frequency (2.5 Hz). The structure of the lungs can be observed, however it is apparent that lung motion at the ventilation frequency resides more strongly at the base of the lung. B) Rendering of the reconstruction at the heart frequency (6.5 Hz) overlaid in red on top of the rendering at the ventilation frequency (2.5 Hz), which is shown in green. The heart rather obviously affects the lung tissue directly adjacent to it and its effect deteriorates with distance from the heart. It can be seen that the apexes of the lung are both affected by the heart due to these regions neighbouring the atria. A modest effect can also be observed at the base of the heart where the ventricles sit against the lung. The analysis for both the heart frequency and ventilation is performed using the same image data.

There is a noticeable effect of the heart directly adjacent to its location, indicating that the physical movement during pumping is a source of cardiogenic oscillations. Due to the different phases of the hearts cycle, there are different regions of lung tissue contracting whilst others are expanding, therefore destructive interference can be generated in the airflow of the lungs. This can cause a mixing of gas between regions of the lung without any noticeable bulk flow of gas at the airway opening. This would be a potentially beneficial mixing mechanism within the lungs, yet it also poses difficulties in determining the behaviour of cardiogenic oscillation when global analysis methods are used. This work has begun to fill the need for techniques that can study the complex and high-speed nature of many physiological functions.

4. CONCLUSION

We have demonstrated a method capable of imaging, analysing and reconstructing the effects of the heart on the lungs with excellent spatial and temporal resolution. Directly adjacent to the heart's location there was considerable motion of lung tissue at the frequency of the heart and this effect diminished distally from the heart. The ventilation frequency was observed throughout the lung yet was seen to be more dominant at the base of the lung. We were able to show that the generation of cardiogenic oscillations can potentially result in destructive interference, making measures at the airway opening incomplete. This method provides the ability to assess the effects of the heart on the lungs, as well as heart health, using synchrotron based X-ray velocimetry methods.

ACKNOWLEDGEMENTS

Support from the Australian Research Council, the National Health and Medical Research Council and the Japan Synchrotron Radiation Research Institute is gratefully acknowledged.

REFERENCES

[1] Pillow, J. J., "High-frequency oscillatory ventilation: mechanisms of gas exchange and lung mechanics," Critical Care Medicine, 33, pp. S135-41 (2005).

[2] Slutsky, A., and Drazen, J. M., "Ventilation With Small Tidal Volumes," New England Journal of Medicine, 347, pp. 630-631 (2002).

[3] Arbour, R., "Cardiogenic Oscillation And Ventilator Autotriggering In Brain-Dead Patients: A Case Series," American Journal of Critical Care, 18, pp. 496-+ (2009).

[4] Lichtwarck-Aschoff, M., Suki, B., Hedlund, A., Sjostrand, U. H., Markstrom, A., Kawati, R., Hedenstierna, G., and Guttmann, J., "Decreasing size of cardiogenic oscillations reflects decreasing compliance of the respiratory system during long-term ventilation," Journal of Applied Physiology, 96, pp. 879-884 (2004).

[5] Wahl, A., Vimlati, L., Moller, K., Schumann, S., Kawati, R., Guttmann, J., and Lichtwarck-Aschoff, M., "Cardiogenic oscillations reflect the compliance of the respiratory system," in *4th European Conference of the International Federation for Medical and Biological Engineering*. vol. 22, J. VanderSloten, P. Verdonck, M. Nyssen, and J. Haueisen, Eds., ed New York: Springer, pp. 2045-2048 (2009).

[6] Schumann, S., Messmer, F., Lichtwarck-Aschoff, M., Haberthuer, C., and Guttmann, J., "Cardiogenic oscillations in spontaneous breathing airway signal reflect respiratory system mechanics," Acta Anaesthesiologica Scandinavica, 55, pp. 980-986 (2011).

[7] Ayappa, I., Norman, R. G., and Rapoport, D. M., "Cardiogenic oscillations on the airflow signal during continuous positive airway pressure as a marker of central apnea," Chest, 116, pp. 660-666 (1999).

[8] Scheuch, G., and Stahlhofen, W., "Effect Of Heart-Rate On Aerosol Recovery And Dispersion In Human Conducting Airways After Periods Of Breathholding," Experimental Lung Research, 17, pp. 763-787 (1991).

[9] Montmerle, S., and Linnarsson, D., "Effects of gravity and blood volume shifts on cardiogenic oscillations in respired gas," Journal of Applied Physiology, 99, pp. 931-936 (2005).

[10] Tusman, G., Suarez-Sipmann, F., Peces-Barba, G., Climente, C., Areta, M., Arenas, P. G., and Bohm, S. H., "Pulmonary blood flow generates cardiogenic oscillations," Respiratory Physiology & Neurobiology, 167, pp. 247-254 (2009).

[11] Maisch, S., Bohm, S. H., Sola, J., Goepfert, M. S., Kubitz, J. C., Richter, H. P., Ridder, J., Goetz, A. E., and Reuter, D. A., "Heart-lung interactions measured by electrical impedance tomography," Critical Care Medicine, 39, pp. 2173-2176 (2011).

[12] Dahlstrom, H., Murphy, J. P., and Roos, A., "Cardiogenic Oscillations In Composition Of Expired Gas - The Pneumocardiogram," Journal of Applied Physiology, 7, pp. 335-339 (1954).

[13] Hathorn, M. K. S., "Cardiac contraction affects respiratory airflow in the term newborn infant," Pediatric Research, 48, pp. 50-57 (2000).

[14] West, J. B., and Hughjones, P., "Pulsatile Gas Flow In Bronchi Caused By Heart Beat," Journal of Applied Physiology, 16, pp. 697-& (1961).

[15] Fouras, A., Allison, B. J., Kitchen, M. J., Dubsky, S., Nguyen, J., Hourigan, K., Siu, K. K. W., Lewis, R. A., Wallace, M. J., and Hooper, S. B., "Altered Lung Motion is a Sensitive Indicator of Regional Lung Disease," Annals of Biomedical Engineering, 40, pp. 1160-1169 (2012).

[16] Dubsky, S., Hooper, S. B., Siu, K. K. W., and Fouras, A., "Synchrotron-based dynamic computed tomography of tissue motion for regional lung function measurement," Journal of the Royal Society Interface, (2012).

[17] Lewis, R. A., Yagi, N., Kitchen, M. J., Morgan, M. J., Paganin, D., Siu, K. K. W., Pavlov, K., Williams, I., Uesugi, K., Wallace, M. J., Hall, C. J., Whitley, J., and Hooper, S. B., "Dynamic imaging of the lungs using x-ray phase contrast," Physics in Medicine and Biology, 50, pp. 5031-5040 (2005).

[18] Thurgood, J., Hooper, S. B., Siew, M., Wallace, M. J., Dubsky, S., Kitchen, M. J., Jamison, R. A., Carnibella, R., and Fouras, A., "Functional Lung Imaging During HFV in Preterm Rabbits," PLoS One - Under Review, (2012).

[19] Fouras, A., Dusting, J., Lewis, R., and Hourigan, K., "Three-dimensional synchrotron x-ray particle image velocimetry," Journal of Applied Physics, 102, (2007).

[20] Fouras, A., Dusting, J., Sheridan, J., Kawahashi, M., Hirahara, H., and Hourigan, K., "Engineering Imaging: Using Particle Image Velocimetry To See Physiology In A New Light," Clinical and Experimental Pharmacology and Physiology, 36, pp. 238-247 (2009).

[21] Kitchen, M. J., Habib, A., Fouras, A., Dubsky, S., Lewis, R. A., Wallace, M. J., and Hooper, S. B., "A new design for high stability pressure-controlled ventilation for small animal lung imaging," Journal of Instrumentation, 5, p. T02002 (2010).

[22] Kitchen, M. J., Lewis, R. A., Morgan, M. J., Wallace, M. J., Siew, M. L., Siu, K. K. W., Habib, A., Fouras, A., Yagi, N., Uesugi, K., and Hooper, S. B., "Dynamic measures of regional lung air volume using phase contrast x-ray imaging," Physics in Medicine and Biology, 53, pp. 6065-6077 (2008).
[23] Fouras, A., Lo Jacono, D., and Hourigan, K., "Target-free Stereo PIV: a novel technique with inherent error estimation and improved accuracy," Experiments in Fluids, 44, pp. 317-329 (2008).
[24] Fouras, A., Dusting, J., and Hourigan, K., "A simple calibration technique for stereoscopic particle image velocimetry," Experiments in Fluids, 42, pp. 799-810 (2007).